

CharDiff-LP: A Diffusion Model with Character-Level Guidance for License Plate Image Restoration*

Kihyun Na^{1[0009-0001-3827-5371]}, Gyuhwan Park^{1[0009-0008-7153-5113]}, and Injung Kim^{1[0000-0003-4439-6097]}

Department of Computer Science and Electrical Engineering, General Graduate School, Handong Global University, Pohang 37554, Republic of Korea
 ijkim@handong.edu
<https://www.csee.kr/gradschool>

Abstract. License plate image restoration is important not only as a preprocessing step for license plate recognition but also for enhancing evidential value, improving visual clarity, and enabling broader reuse of license plate images. We propose a novel diffusion-based framework with character-level guidance, CharDiff-LP, which effectively restores and recognizes severely degraded license plate images captured under realistic conditions. CharDiff-LP leverages fine-grained character-level priors extracted through external segmentation and Optical Character Recognition (OCR) modules tailored for low-quality license plate images. For precise and focused guidance, CharDiff-LP incorporates a novel *Character-guided Attention through Region-wise Masking (CHARM)* module, which ensures that each character’s guidance is restricted to its own region, thereby avoiding interference with other regions. In experiments, CharDiff-LP significantly outperformed baseline restoration models in both restoration quality and recognition accuracy, achieving a 28.3% relative reduction in character error rate (CER) on the Roboflow-LP dataset compared with the best-performing baseline.

Keywords: License Plate Recognition · License Plate Image Restoration · Scene Text Image Super-Resolution · Diffusion Models

1 Introduction

License Plate Recognition (LPR) is a core component of intelligent transportation systems (ITS), supporting applications such as traffic surveillance, automated toll collection, and access control. In practice, however, license plate images acquired in real-world environments often suffer from low resolution, motion blur, compression artifacts, and adverse lighting, which substantially deteriorate the performance of LPR systems [7, 17].

To alleviate this, previous work has explored image restoration techniques [4, 43, 37, 39, 41, 13] as a preprocessing step for LPR. Beyond boosting recognition

* Corresponding author: Injung Kim (ijkim@handong.edu).

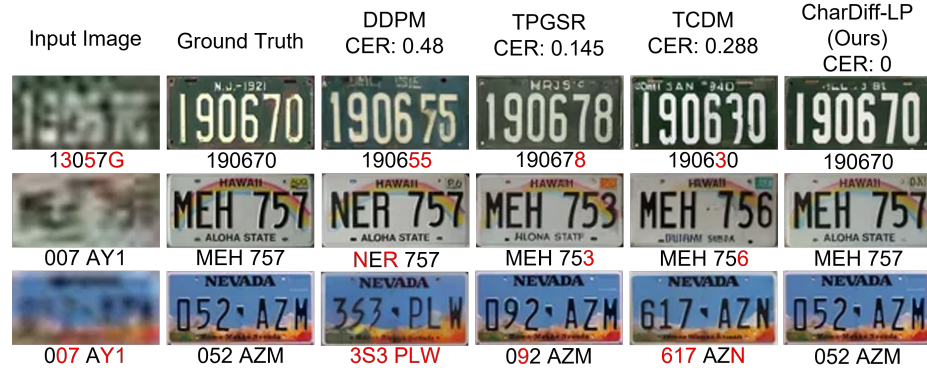


Fig. 1. The results of diffusion-based image restoration models on severely degraded license plate images. Characters in red font indicate erroneously recognized and incorrectly restored characters (CER: character error rate).

accuracy, license plate restoration is also important for verifying recognition results, increasing evidential value, and improving the visual clarity of interfaces such as advanced driver assistance systems (ADAS). GAN-based [16, 12, 14] and more recent diffusion-based restoration models [1, 5] have shown substantial improvements. However, these methods do not explicitly exploit the textual information of license plates and, under severe degradation, often synthesize images that fail to preserve proper character shapes or even resemble different characters, as illustrated in Fig. 1.

Several studies introduced text-guided restoration techniques into the LPR domain by designing loss functions that leverage OCR outputs during training [11, 24, 28, 25]. Although such training-time guidance improves restoration performance to some extent, the model still lacks explicit inference-time guidance regarding character identities and locations, which limits its effectiveness in restoring fine details under severe degradation.

In the field of scene text image super-resolution (STISR), recent models employ conditional diffusion guided by textual information extracted from the input image [44, 26, 32]. Because they guide the denoising process via global cross-attention, these methods do not fully exploit the spatial information of individual characters. As a result, each character-specific prior may not focus exclusively on its corresponding region, causing interference across neighboring regions. Moreover, these STISR models are not tailored to the structured and highly constrained nature of license plates.

To address these limitations, we propose *CharDiff-LP*, a diffusion-based framework with inference-time character-level guidance for restoring and recognizing low-quality license plate images. CharDiff-LP integrates fine-grained character-level priors extracted by three modules specialized for low-quality license plates: an external character segmentation module, an OCR model robust to degraded inputs, and a character encoder that converts individual characters into embeddings. The segmentation module leverages the structural format of license

plates to identify character regions, the OCR model is trained on heavily degraded images, and the character encoder provides more fine-grained features than conventional string-level text encoders.

A key component of our framework is the Character-guided Attention through Region-wise Masking (CHARM) module, which applies spatially masked cross-attention so that each character embedding attends only to its corresponding region, preventing inter-character interference. To the best of our knowledge, this is the first diffusion-based license plate restoration model to incorporate character-level guidance via spatially masked cross-attention.

We validate our framework on two LPR datasets: one with paired high- and low-quality images generated via synthetic degradations, and another with real low-quality dashcam images without high-quality counterparts. In experiments, CharDiff-LP consistently improved both restoration quality and text recognition accuracy over recently developed baseline models. On the Roboflow-LP dataset, it reduced the CER from 11.3% to 8.1% compared to the second-best model, TCDM [26], corresponding to a 28.3% relative error reduction. These results demonstrate that incorporating character-level priors with spatially guided attention is highly effective for restoring severely degraded images in practical LPR scenarios.

Our main contributions are summarized as follows:

- **CharDiff-LP:** We propose a diffusion-based framework tailored for license plate restoration and recognition, which incorporates character-level priors to guide the restoration process.
- **CHARM:** We introduce the Character-guided Attention through Region-wise Masking (CHARM) module, which injects individual character embeddings into their corresponding regions via masked cross-attention, preventing interference between neighboring characters.
- **Comprehensive Evaluation:** We conduct extensive experiments on two license plate datasets and show that CharDiff-LP outperforms baselines in both perceptual quality and character-level recognition metrics, especially under severe real-world degradations.

2 Related Work

2.1 License Plate Restoration and Recognition

Traditional LPR systems typically follow a two-stage pipeline of license plate detection and character recognition, and operate directly on the captured image without explicit restoration [31, 10, 22]. Under realistic conditions, however, degradations such as low resolution, motion blur, and sensor noise lead to large drops in accuracy [30, 8, 15, 19, 23].

To mitigate this, many studies add an image restoration stage before recognition. In general, unconditional restoration methods treat license plate images as generic images and learn a mapping from low- to high-quality images using

CNN- or GAN-based restoration [40, 33, 9, 16, 12, 14] or more recent diffusion-based restoration [1, 5]. These methods improve visual quality but do not explicitly leverage textual content, and under severe degradation they may hallucinate semantically or structurally incorrect characters. Text-guided methods incorporate OCR feedback via semantic supervision or OCR-based losses and discriminators [45, 11, 24, 28, 25]. However, they mainly use text priors as training-time regularizers and still lack explicit, localized guidance at inference time.

2.2 Scene Text Image Super-Resolution

STISR shares similar goals with license plate restoration: enhancing both visual quality and text legibility. TSRN [35] introduced a text-specific architecture with sequential residual blocks and a boundary-aware loss, highlighting the gap between synthetic and real-world degradations. Subsequent works leveraged pre-trained recognizers to provide auxiliary OCR losses [3], but guidance was still absent at inference time. TPGSR [20] first introduced inference-time guidance by fusing a text prior from a recognizer with image features, and TATT [21] replaced local fusion with Transformer-based cross-attention for global string-level alignment. More recently, diffusion-based STISR models such as TCDM [26] and DCDM [32] inject textual information directly into the denoising process, but rely on global cross-attention and do not explicitly constrain each character prior to its spatial region.

Motivated by these limitations, we extend text-guided diffusion models from STISR to the LPR domain with two key enhancements. First, we extract reliable character-level priors using an external segmentation module and an OCR model specialized for degraded license plate images. Second, we introduce the CHARM module, which injects character embeddings via region-wise masked cross-attention so that each prior focuses on its corresponding character region. To the best of our knowledge, CharDiff-LP is the first diffusion-based license plate restoration model with explicitly localized, character-level guidance.

3 Method

3.1 Overview

Figure 2 illustrates the overall process of the CharDiff-LP framework, which aims to restore a low-quality license plate (LP) image by incorporating fine-grained character-level guidance into the denoising process.

Given a low-quality input image x^{LQ} , CharDiff-LP segments individual characters with an external segmentation module customized for license plate images. Then, a robust OCR model recognizes the segmented character images.

Subsequently, CharDiff-LP exploits two kinds of contextual information: a sequence of recognized characters $\mathbf{y} = (y_1, \dots, y_n)$, and their corresponding bounding boxes $\mathbf{B} = (B_1, \dots, B_n)$. y_i 's are converted into the corresponding character embeddings e_i 's through the character encoder. The bounding boxes are converted into binary spatial masks $\mathbf{M} = (M_1, \dots, M_n)$, $M_i \in \{0, 1\}^{H \times W}$, where

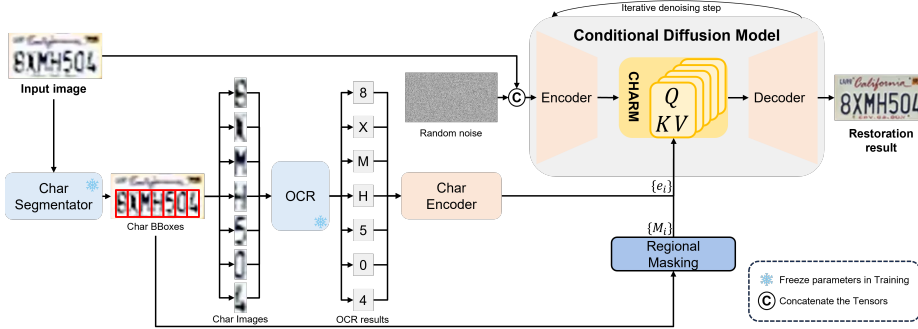


Fig. 2. The overview of the CharDiff-LP framework. Character-level priors—character embeddings and spatial masks—are extracted from the low-quality input image using external segmentation and OCR modules. These priors are then injected into the diffusion model via the CHARM module to guide the restoration process at the character level throughout the denoising process.

$H \times W$ denotes the feature map size. $M_i[u, v]$ is one for $(u, v) \in B_i$ and zero for other elements. The prior from each character consists of the character embedding extracted from the character class and the binary mask derived from its region, i.e., $c_i = (e_i, M_i)$.

The restoration process is based on a diffusion model employing a U-Net architecture. The character-level priors (c_1, \dots, c_n) are referenced through the CHARM module, which is placed in the middle of the U-Net. In the cross-attention mechanism of the CHARM module, the attention weight for referencing each character’s prior incorporates the spatial mask M_i , ensuring that the embedding e_i from the i -th character guides only its corresponding region.

CharDiff-LP combines two types of contextual information: the global image context from the low-quality image x^{LQ} and the local context from the character-level priors $\{c_i\}_{i=1}^n$. Therefore, CharDiff-LP is capable of generating high-quality images that remain consistent with the input while accurately preserving the unique features of each character. A detailed explanation of each step is provided in the following subsections.

3.2 Diffusion-based Restoration Model

We design our restoration model based on the denoising diffusion probabilistic model (DDPM) [6]. Let x_0 denote a high-quality training image and x_t its noisy version at timestep t . During training, the forward diffusion process degrades the training samples by adding noise ϵ , as shown in Eq. 1:

$$x_t = \sqrt{\bar{\alpha}_t}x_0 + \sqrt{1 - \bar{\alpha}_t}\epsilon, \quad \epsilon \sim \mathcal{N}(0, I), \quad (1)$$

The noise predictor $\epsilon_\theta(x'_t, t, c)$ is then trained to estimate the noise ϵ from the noisy image x'_t and the conditioning information c at each timestep, as defined in Eq. 2:

$$\mathcal{L}_{\text{cond}} = \mathbb{E}_{x_0, \epsilon, t} \left[|\epsilon - \epsilon_\theta(x'_t, t, c)|_2^2 \right]. \quad (2)$$

During restoration, the model progressively reconstructs a high-quality image from x_t using the estimated noise. In our study, the conditioning information c consists of a low-quality input image x^{LQ} and textual priors. The former is concatenated with x_t to form $x'_t = \text{Concat}(x_t, x^{LQ})$, while the latter is incorporated into the denoising process via cross-attention to guide the restoration process.

In this study, we compare three settings with respect to the text prior. The first setting, *no text prior*, uses $c = \emptyset$, where the model relies solely on x^{LQ} , corresponding to the DDPM baseline. The second setting, *string-level prior*, employs a single embedding for the entire string, $c = e_y$, similar to TCDM [26]. The third setting, *character-level prior (proposed)*, introduces a set of localized priors, $c = \{(e_i, M_i)\}_{i=1}^n$, where each pair encodes the identity and spatial region of a character. Following TCDM, the text priors c are injected into the middle block of the U-Net backbone in the second and third settings. The character-level priors are spatially localized via binary masks M_i , enabling more precise guidance for individual character regions.

3.3 Character-Level Prior

We construct character-level priors from the low-quality license plate image x^{LQ} , which consist of semantic embeddings and spatial masks for individual characters, denoted as $\{(e_i, M_i)\}_{i=1}^n$. The extraction process comprises three stages: character segmentation, character recognition, and embedding projection.

(1) Character Segmentation and Mask Generation To localize character regions, we utilize a CRAFT-based text detector [2] fine-tuned on an internal license plate dataset collected from [29] that is independent of Roboflow-LP and Dashcam-LP. The detector outputs quadrilateral character regions, which are converted into axis-aligned bounding boxes $\{B_i\}$ through post-processing. For each bounding box, we generate a binary mask $M_i \in \{0, 1\}^{H \times W}$, where only the elements inside the region are set to one. These masks are resized to match the resolution of the U-Net feature map used in the CHARM module. The segmentation module is frozen during training.

(2) Character Recognition We crop the segmented character regions and feed them to the OCR module to predict their class labels. We adopt MGP-STR [34], a strong scene-text recognizer, as the OCR module. To improve robustness to low-quality inputs, we further fine-tune it on artificially degraded license plate images, and keep the OCR model frozen during the training of the diffusion model.

(3) Character Embedding The recognized character labels are one-hot encoded, and then converted into character embeddings $\{e_i\}_{i=1}^n$ by a lightweight Transformer encoder. Unlike the previous two modules, the embedding module is trained jointly with the diffusion model, allowing it to learn task-specific representations to guide the restoration process.

Consequently, CharDiff-LP extracts a set of localized priors that encode both the class and spatial location M_i of each character. These priors are delivered to the CHARM module to enable spatially focused and semantically informed image restoration.

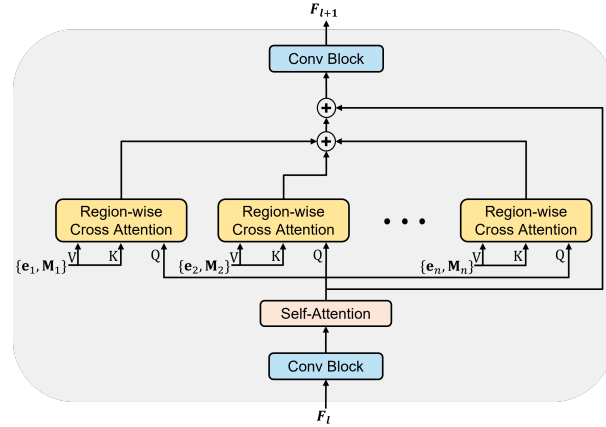


Fig. 3. The detailed architecture of the CHARM module. Given a feature map F_l from the U-Net encoder, the CHARM module injects the character embedding e_i of each character only to the designated spatial region using the spatial mask M_i via masked cross-attention.

3.4 Character-guided Attention through Region-wise Masking (CHARM)

To inject character-level priors into the denoising process, we replace the standard string-level cross-attention in the U-Net middle block with the Character-guided Attention through Region-wise Masking (CHARM) module, a lightweight yet effective mechanism for spatially localized attention. The CHARM module combines the character embeddings e_i with the intermediate feature map through masked cross-attention, as shown in Fig. 3.

Feature Preparation: Let $F_l \in \mathbb{R}^{C \times H \times W}$ denote the input feature map of the CHARM module. We first flatten the spatial dimensions and apply a linear projection to obtain the query matrix $Q \in \mathbb{R}^{C \times HW}$. Each character embedding $e_i \in \mathbb{R}^C$ is expanded to form key and value vectors $K_i, V_i \in \mathbb{R}^{C \times 1}$ via 1D convolution or linear layers.

Region-masked Cross-Attention: For the i^{th} character, we compute attention weights between the query Q and the key K_i , applying a spatial mask $M_i \in \{0, 1\}^{H \times W}$, which is flattened to a vector in $\{0, 1\}^{HW}$ during computation (we reuse the same symbol M_i by slight abuse of notation). Let the channel dimension be d (i.e., $Q \in \mathbb{R}^{d \times HW}$, $K_i, V_i \in \mathbb{R}^{d \times 1}$). We first compute the masked attention as

$$A_i = \text{softmax} \left(\frac{Q^\top K_i}{\sqrt{d}} + (1 - M_i) \cdot (-\infty) \right), \quad (3)$$

where $A_i \in \mathbb{R}^{HW}$. Here, the term $(1 - M_i) \cdot (-\infty)$ serves as a masking operation, effectively setting the attention scores of background regions to zero after the softmax operation.¹ The attended feature $h_i \in \mathbb{R}^{d \times HW}$ is then computed as

$$h_i = V_i \cdot A_i^\top, \quad (4)$$

¹ In practice, $-\infty$ is implemented as a large negative constant.

and reshaped back to $\mathbb{R}^{d \times H \times W}$. Finally, the features from all characters are aggregated and added to the input feature map F_l via a residual connection:

$$F_{l+1} = F_l + \sum_{i=1}^n \text{Reshape}(h_i). \quad (5)$$

4 Experiments

4.1 Datasets

We evaluate CharDiff-LP on two license plate datasets: Roboflow-LP and Dashcam-LP. Roboflow-LP contains 4,000 high-quality images from Roboflow Universe [27]; their low-quality counterparts were artificially generated using an extended Real-ESRGAN degradation pipeline [36] with additional perspective, contrast, and motion-blur augmentations to better mimic dashcam footage. The dataset is split into training, validation, and test sets with a 7:2:1 ratio.

Dashcam-LP comprises 10,000 images captured from vehicle dashcams under diverse driving conditions. Among them, 9,000 relatively clean images are used as high-quality training targets, and 1,000 challenging low-quality images (e.g., long distances, strong motion blur) are used as an unpaired real-world test set without corresponding high-quality references. For training, low-quality counterparts of the high-quality images are synthesized using the same degradation pipeline as in Roboflow-LP. We train separate models on the training splits of Roboflow-LP and Dashcam-LP and evaluate them on the corresponding test splits.

String-level annotations are available for all images, enabling recognition evaluation (CER and plate-level accuracy) even for unpaired real-world low-quality test images without corresponding high-quality references.

4.2 Evaluation Metrics

We evaluate both restoration quality and downstream recognition performance. On the Roboflow-LP dataset, where paired high-quality images are available, we measure PSNR, SSIM [38], and LPIPS [42] between the restored images and the ground-truth references. For license plate recognition (LPR), we compute the character error rate (CER) and plate-level accuracy based on exact string matching. Recognition performance on both Roboflow-LP and Dashcam-LP is evaluated by feeding the restored images into a fixed (frozen) MGP-STR recognizer; this recognizer is used solely for evaluation and is not jointly trained with any restoration model.

4.3 Baseline Models

We compared CharDiff-LP with three representative baseline models: (i) DDPM [6], a conditional diffusion model that takes only a low-quality image as input and serves as an unguided diffusion baseline; (ii) TPGSR [20], a general STISR

Table 1. Quantitative evaluation results on the **Roboflow-LP** test set (paired real HQ and synthetic LQ images). CharDiff-LP achieves the best performance across all restoration and recognition metrics. Boldface indicates the best performance. (FT: fine-tuning, LPI: license plate images.)

Method	Trained on LPI	PSNR \uparrow	SSIM \uparrow	LPIPS \downarrow	CER \downarrow	LPR Acc. \uparrow
DDPM (no text prior)	Yes	23.98	0.8363	0.5022	0.212	0.514
TPGSR (pretrained)	No	18.85	0.6463	0.6221	0.425	0.458
TPGSR (FT)	Yes	23.75	0.8216	0.4340	0.157	0.637
TCDM (pretrained)	No	18.91	0.6461	0.6124	0.404	0.476
TCDM (FT)	Yes	24.16	0.8411	0.4114	0.113	0.667
CharDiff-LP (Ours)	Yes	24.35	0.8487	0.3832	0.081	0.697

Table 2. Quantitative evaluation results on the **Dashcam-LP** test set (unpaired real LQ images). CharDiff-LP achieves the best performance in both metrics. Boldface indicates the best performance. (FT: fine-tuning, LPI: license plate images.)

Method	Trained on LPI	CER \downarrow	LPR Acc. \uparrow
DDPM (No text prior)	Yes	0.2118	0.5458
TPGSR (pretrained)	No	0.4473	0.2226
TPGSR (FT)	Yes	0.1714	0.6266
TCDM (pretrained)	No	0.4339	0.2327
TCDM (FT)	Yes	0.1613	0.6367
CharDiff-LP (Ours)	Yes	0.1512	0.6965

method that leverages textual priors extracted by a recognizer and incorporates them via local feature fusion; and (iii) TCDM [26], a diffusion-based STISR model that injects string-level textual priors into the denoising process through global cross-attention. For TPGSR and TCDM, we evaluated both the official pretrained models and variants fine-tuned on our license plate datasets. DDPM and CharDiff-LP were trained from scratch on each dataset. We also considered DiffPlate [1] and LP-Diff [5], but excluded them from comparisons because they do not provide official implementations or adopt settings that are not directly comparable, such as multi-frame inputs.

4.4 Implementation Details

CharDiff-LP was implemented in PyTorch based on the DDPM framework [6]. We used 1,000 diffusion steps with a linear noise schedule during training and 50 steps for inference. The noise predictor was optimized with the loss in Eq. 2 using AdamW [18] with a batch size of 64, a fixed learning rate of 3×10^{-4} , and 100k training steps. All input images were resized to 96×48 pixels, reflecting the typical aspect ratio of U.S. license plates. For all methods, we followed the original implementation details when available and trained on a single NVIDIA RTX 4090 GPU under identical data splits and evaluation protocols.

4.5 Comparison with Baseline Models

Quantitative Evaluation on Roboflow-LP We evaluated CharDiff-LP using both restoration metrics (PSNR, SSIM [38], and LPIPS [42]) and recognition

metrics (CER and LPR accuracy), and compared it against the baseline models. Table 1 presents the evaluation results on the Roboflow-LP dataset, whose test set consists of pairs of real HQ and synthetic LQ images. The real HQ images were used as ground truth to compute the restoration metrics. ‘Trained on LPI’ indicates that the model was trained or fine-tuned on the license plate image dataset, Roboflow-LP, starting from its pretrained weights. DDPM and CharDiff-LP were trained from scratch without any pretraining, using only LPI data.

In Table 1, the proposed model, CharDiff-LP, demonstrates superior performance across all metrics. Compared to the strongest baseline, TCDM (FT), CharDiff-LP improves PSNR by 0.19 dB, SSIM by 0.0076, and LPIPS by 0.0282. In addition, CharDiff-LP outperforms the baseline models in terms of recognition performance. Compared to the second-best model, TCDM (FT), CharDiff-LP reduces the Character Error Rate (CER) from 11.3% to 8.1%, corresponding to an absolute improvement of 3.2 percentage points and a relative error reduction of 28.3%. It also achieves the highest plate-level LPR accuracy of 69.7%. Given the poor quality of the test images (as shown in Fig. 4), these results demonstrate that the proposed character-level prior is highly effective in restoring global structure—crucial for identity preservation—as well as fine-grained details.

Quantitative Evaluation on Dashcam-LP To assess generalization to authentic and uncontrolled degradations, we also evaluated recognition performance on the Dashcam-LP test set, which contains real low-quality images without high-quality counterparts (Table 2). ‘Trained on LPI’ indicates trained or fine-tuned on the Dashcam-LP training split. Trained only on this dataset, CharDiff-LP still achieves the best performance, reducing CER from 16.1% to 15.1% compared to TCDM (FT) and improving plate-level LPR accuracy from 63.7% to 69.7% (a gain of 6.0 percentage points). These results confirm that the proposed character-level guidance is robust to challenging, unseen real-world degradation patterns.

Qualitative Evaluation Fig. 4 and 5 illustrate the restoration results on samples from the Roboflow-LP and Dashcam-LP test sets. All methods enhance the perceptual quality of low-quality inputs, but the baseline models often produced artifacts, distorted character shapes, or identity changes (e.g., ‘I→T’, ‘7→3’, ‘B→8’ in Fig. 4). In contrast, CharDiff-LP generally yielded cleaner character shapes and better preserved the ground-truth identities across both synthetic and real-world degradations, which is consistent with the quantitative gains in CER and plate-level accuracy. Failure cases predominantly arise when the input is severely degraded, rendering reliable character recovery infeasible for all methods.

4.6 Ablation Studies

To assess the contribution of each design choice in CharDiff-LP, we conducted ablation experiments on three components: (1) the use of text priors, (2) the



Fig. 4. Restoration results on low-quality test images from the **Roboflow-LP** dataset. Red fonts indicate incorrectly restored characters and misrecognition results.

Table 3. The results of ablation studies on the **Roboflow-LP** dataset (paired real HQ and synthetic LQ images), showing that each component incrementally improves restoration and recognition performance.

Method Variant	PSNR↑	SSIM↑	LPIPS↓	CER↓	LPR Acc.↑
DDPM (no text prior)	23.98	0.8363	0.5022	0.2118	0.514
DDPM + String-level prior	24.21	0.8415	0.4478	0.1539	0.575
DDPM + Character-level prior	24.30	0.8492	0.4210	0.1187	0.621
CharDiff-LP (Ours)	24.35	0.8487	0.3832	0.0810	0.697

granularity of guidance (string-level vs. character-level), and (3) the CHARM masking strategy. All variants were trained from scratch on the synthetic training set and evaluated on both Roboflow-LP and Dashcam-LP.

In Tables 3 and 4, the model without any text prior performs worst, indicating the importance of textual guidance. Adding a string-level prior yields a substantial gain in CER and plate-level accuracy, and replacing it with character-level priors further improves both restoration and recognition metrics, suggesting that localized guidance helps recover fine details. The full CharDiff-LP with CHARM achieves the best overall performance and generalizes best to Dashcam-LP, demonstrating that region-wise masking effectively prevents interference between characters.

For further analysis, we visualized attention maps in the U-Net middle block to compare string-level and character-level guidance (Fig. 6). With string-level priors, attention tends to be diffuse and often spills over into neighboring characters, potentially leading to identity confusion. In contrast, CharDiff-LP yields sharp and well-localized attention that is confined to individual character regions, suggesting that CHARM effectively enforces spatially disentangled guidance and helps explain the performance gains observed in our ablation studies.

GT Label	724 ZRM	1A MOA3U	G57 9FL	825 S80	CS 40208	32H 394	V39 1028
Input image							
	724 ZRM	1A MOA3U	G57 9FL	825 S80	CS 40208	32H 394	V39 1028
DDPM							
	724 1V9	1A 6TA	557 9FL	935 591	CY VBO	621 391	V3Y 112X
TPGSR							
	724 ZWN	1A MOA38	657 9FL	F35 563	C9 40208	3ZH 394	U39 1028
TCDM							
	724 ZRN	1A MOA38	G57 9FL	825 580	CS 40208	J2H 394	N39 1028
CharDiff-LP (Ours)							
	724 ZRM	1A MOA3U	G57 9FL	825 S80	CS 40208	32H 394	V39 1028

Fig. 5. Restoration results of low-quality test images from the **Dashcam-LP** dataset. Red fonts indicate incorrectly restored characters and misrecognition results.

Table 4. The results of ablation studies on the **Dashcam-LP** dataset (unpaired real LQ images), showing that each component incrementally improves recognition performance.

Method Variant	CER \downarrow	LPR Acc. \uparrow
DDPM (no text prior)	0.2118	0.5458
DDPM + String-level prior	0.1709	0.6534
DDPM + Character-level prior	0.1614	0.6703
CharDiff-LP (Ours)	0.1512	0.6965

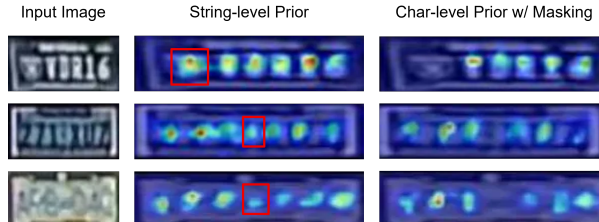


Fig. 6. Cross-attention maps from the U-Net middle block comparing string-level priors and our character-level prior with CHARM. String-level priors often attend to non-character regions, whereas CHARM concentrates attention on the character masks.

5 Conclusion

We presented CharDiff-LP, a diffusion-based license plate image restoration and recognition model that leverages character-level priors. Character masks from the segmentation module and character labels predicted by the OCR module are converted into embeddings by a character encoder, and injected into the diffusion U-Net via the CHARM module, which applies masked cross-attention to guide each character region separately.

In experiments on two license plate image datasets, the proposed model, CharDiff-LP, consistently improved PSNR, SSIM, LPIPS, and recognition metrics over recent text-guided baselines. On Roboflow-LP, CharDiff-LP reduced CER from 11.3% to 8.1% and achieved the highest plate-level accuracy; similar gains were observed on the real-world Dashcam-LP test set.

A limitation of our model lies in its reliance on external segmentation and OCR modules: severe recognition errors may result in visually plausible yet semantically incorrect restorations. In safety-critical applications, this issue can be mitigated by presenting multiple restoration candidates alongside the original footage and discarding highly ambiguous cases. Future work includes jointly training the recognition and restoration modules, as well as incorporating more principled uncertainty modeling to enable trustworthy deployment.

References

1. AlHalawani, S., Benjdira, B., Ammar, A., Koubaa, A., Ali, A.M.: DiffPlate: A diffusion model for super-resolution of license plate images. *Electronics* **13**(13) (2024). <https://doi.org/10.3390/electronics13132670>
2. Baek, Y., Lee, B., Han, D., Yun, S., Lee, H.: Character region awareness for text detection. In: in Proc. IEEE Conf. Comput. Vis. Pattern Recognit. (CVPR). pp. 9365–9374 (2019)
3. Chen, J., Li, B., Xue, X.: Scene text telescope: Text-focused scene image super-resolution. In: in Proc. IEEE Conf. Comput. Vis. Pattern Recognit. (CVPR). pp. 12026–12035 (2021)
4. Dong, C., Loy, C.C., He, K., Tang, X.: Image super-resolution using deep convolutional networks. In: in Proc. IEEE Conf. Comput. Vis. Pattern Recognit. (CVPR). pp. 189–197 (2015)
5. Gong, H., Zhang, Z., Feng, Y., Nguyen, A., Liu, H.: LP-Diff: Towards improved restoration of real-world degraded license plate. In: in Proc. IEEE Conf. Comput. Vis. Pattern Recognit. (CVPR). pp. 17831–17840 (2025)
6. Ho, J., Jain, A., Abbeel, P.: Denoising diffusion probabilistic models. *Adv. Neural Inf. Process. Syst.* **33**, 6840–6851 (2020)
7. Kaiser, P., Schirrmacher, F., Lorch, B., Riess, C.: Learning to decipher license plates in severely degraded images. In: in Proc. Int. Conf. Pattern Recognit. (ICPR). pp. 544–559 (2021)
8. Ke, X., Zeng, G., Guo, W.: An ultra-fast automatic license plate recognition approach for unconstrained scenarios. *IEEE Trans. Intell. Transp. Syst.* **24**(5), 5172–5185 (2023)
9. Kim, D., Kim, J., Park, E.: AFA-Net: Adaptive feature attention network in image deblurring and super-resolution for improving license plate recognition. *Comput. Vis. Image Underst.* **238**, 103879 (2024)
10. Laroca, R., Zanlorensi, L.A., Gonçalves, G.R., Todt, E., Schwartz, W.R., Menotti, D.: An efficient and layout-independent automatic license plate recognition system based on the YOLO detector. *IET Intell. Transp. Syst.* **15**(4), 483–503 (2021)
11. Lee, S., Kim, J.H., Heo, J.P.: Super-resolution of license plate images via character-based perceptual loss. In: in Proc. IEEE Int. Conf. Big Data Smart Comput. (Big-Comp). pp. 560–563 (2020)

12. Lee, Y., Yun, J., Hong, Y., Lee, J., Jeon, M.: Accurate license plate recognition and super-resolution using a generative adversarial networks on traffic surveillance video. In: in Proc. IEEE Int. Conf. Consum. Electron. Asia (ICCE-Asia). pp. 1–4 (2018). <https://doi.org/10.1109/ICCE-ASIA.2018.8552121>
13. Li, H., Yang, Y., Chang, M., Chen, S., Feng, H., Xu, Z., Li, Q., Chen, Y.: SRDiff: Single image super-resolution with diffusion probabilistic models. *Neurocomputing* **479**, 47–59 (2022)
14. Lin, M., Liu, L., Wang, F., Li, J., Pan, J.: License plate image reconstruction based on generative adversarial networks. *Remote Sens.* **13**(15), 3018 (2021). <https://doi.org/10.3390/rs13153018>
15. Liu, Q., Liu, Y., Chen, S.L., Zhang, T.H., Chen, F., Yin, X.C.: Improving multi-type license plate recognition via learning globally and contrastively. *IEEE Trans. Intell. Transp. Syst.* **25**(9), 11092–11102 (2024)
16. Liu, W., Liu, X., Ma, H., Cheng, P.: Beyond human-level license plate super-resolution with progressive vehicle search and domain priori GAN. In: in Proc. ACM Int. Conf. Multimedia (ACM MM). pp. 1618–1626 (2017). <https://doi.org/10.1145/3123266.3123422>
17. Liu, Y.Y., Liu, Q., Chen, S.L., Chen, F., Yin, X.C.: Irregular license plate recognition via global information integration. In: in Proc. Int. Conf. Multimedia Model. pp. 325–339 (2024)
18. Loshchilov, I., Hutter, F.: Decoupled weight decay regularization. arXiv preprint arXiv:1711.05101 (2017)
19. Luo, X., Huang, Y., Miao, W.: Real-world license plate image super-resolution via domain-specific degradation modeling. In: in Proc. IEEE Conf. Artif. Intell. (CAI). pp. 1175–1180 (2024)
20. Ma, J., Guo, S., Zhang, L.: Text prior guided scene text image super-resolution. *IEEE Trans. Image Process.* **32**, 1341–1353 (2023)
21. Ma, J., Liang, Z., Zhang, L.: A text attention network for spatial deformation robust scene text image super-resolution. In: in Proc. IEEE Conf. Comput. Vis. Pattern Recognit. (CVPR). pp. 5911–5920 (2022)
22. Moussa, D., Maier, A., Spruck, A., Seiler, J., Riess, C.: Forensic license plate recognition with compression-informed transformers. In: in Proc. IEEE Int. Conf. Image Process. (ICIP). pp. 406–410 (2022)
23. Na, K., Oh, J., Cho, Y., Kim, B., Cho, S., Choi, J., Kim, I.: MF-LPR2: Multi-frame license plate image restoration and recognition using optical flow. *Comput. Vis. Image Underst.* **256**, 104361 (2025)
24. Nascimento, V., Laroca, R., Lambert, J.d.A., Schwartz, W.R., Menotti, D.: Super-resolution of license plate images using attention modules and sub-pixel convolution layers. *Comput. Graph.* **113**, 69–76 (2023)
25. Nascimento, V., Laroca, R., Ribeiro, R.O., Schwartz, W.R., Menotti, D.: Enhancing license plate super-resolution: A layout-aware and character-driven approach. In: in Proc. SIBGRAPI Conf. Graphics, Patterns Images. pp. 1–6 (2024). <https://doi.org/10.1109/SIBGRAPI62404.2024.10716303>
26. Noguchi, C., Fukuda, S., Yamanaka, M.: Scene text image super-resolution based on text-conditional diffusion models. In: in Proc. IEEE Winter Conf. Appl. Comput. Vis. (WACV). pp. 1485–1495 (2024)
27. openAICLIP: Plate types dataset. <https://universe.roboflow.com/openaiclip/plate-types-dgw88> (Jul 2023)
28. Pan, Y., Tang, J., Tjahjadi, T.: LPSRGAN: Generative adversarial networks for super-resolution of license plate image. *Neurocomputing* **580**, 127426 (2024)

29. PlatesMania: License-plate photo archive. <https://platesmania.com/> (2025)
30. Silva, S.M., Jung, C.R.: A flexible approach for automatic license plate recognition in unconstrained scenarios. *IEEE Trans. Intell. Transp. Syst.* **23**(6), 5693–5703 (2021)
31. Silva, S.M., Jung, C.R.: License plate detection and recognition in unconstrained scenarios. In: in Proc. Eur. Conf. Comput. Vis. (ECCV). pp. 580–596 (2018)
32. Singh, S., Keserwani, P., Iwamura, M., Roy, P.P.: DCDM: Diffusion-conditioned-diffusion model for scene text image super-resolution. In: in Proc. Eur. Conf. Comput. Vis. (ECCV). pp. 303–320 (2024)
33. Vasek, V., Franc, V., Urban, M.: License plate recognition and super-resolution from low-resolution videos by convolutional neural networks. In: in Proc. Brit. Mach. Vis. Conf. (BMVC). p. 132 (2018)
34. Wang, P., Da, C., Yao, C.: Multi-granularity prediction for scene text recognition. In: in Proc. Eur. Conf. Comput. Vis. (ECCV). pp. 339–355 (2022)
35. Wang, W., Xie, E., Liu, X., Wang, W., Liang, D., Shen, C., Bai, X.: Scene text image super-resolution in the wild. In: in Proc. Eur. Conf. Comput. Vis. (ECCV). pp. 650–666 (2020)
36. Wang, X., Xie, L., Dong, C., Shan, Y.: Real-ESRGAN: Training real-world blind super-resolution with pure synthetic data. In: in Proc. IEEE Int. Conf. Comput. Vis. Workshops (ICCVW). pp. 1905–1914 (2021)
37. Wang, X., Yu, K., Wu, S., Gu, J., Liu, Y., Dong, C., Qiao, Y., Loy, C.C.: ESRGAN: Enhanced super-resolution generative adversarial networks. In: in Proc. Eur. Conf. Comput. Vis. Workshops (ECCVW). pp. 630–645 (Sep 2018)
38. Wang, Z., Bovik, A.C., Sheikh, H.R., Simoncelli, E.P.: Image quality assessment: From error visibility to structural similarity. *IEEE Trans. Image Process.* **13**(4), 600–612 (2004)
39. Yang, F., Yang, H., Fu, J., Lu, H., Guo, B.: Learning texture transformer network for image super-resolution. In: in Proc. IEEE Conf. Comput. Vis. Pattern Recognit. (CVPR). pp. 5791–5800 (Jun 2020)
40. Yang, Y., Bi, P., Liu, Y.: License plate image super-resolution based on convolutional neural network. In: in Proc. IEEE Int. Conf. Image, Vis. Comput. (ICIWC). pp. 723–727 (2018)
41. Zamir, S.W., Arora, A., Khan, S., Hayat, M., Khan, F.S., Yang, M.H.: Restormer: Efficient transformer for high-resolution image restoration. In: in Proc. IEEE Conf. Comput. Vis. Pattern Recognit. (CVPR). pp. 5728–5739 (2022)
42. Zhang, R., Isola, P., Efros, A.A., Shechtman, E., Wang, O.: The unreasonable effectiveness of deep features as a perceptual metric. In: in Proc. IEEE Conf. Comput. Vis. Pattern Recognit. (CVPR). pp. 586–595 (2018)
43. Zhang, Y., Tian, Y., Kong, Y., Zhong, B., Fu, Y.: Residual dense network for image super-resolution. In: in Proc. IEEE Conf. Comput. Vis. Pattern Recognit. (CVPR). pp. 2472–2481 (2018)
44. Zhou, Y., Gao, L., Tang, Z., Wei, B.: Recognition-guided diffusion model for scene text image super-resolution. In: in Proc. IEEE Int. Conf. Acoust., Speech Signal Process. (ICASSP). pp. 1–5 (2023)
45. Zou, Y., Wang, Y., Guan, W., Wang, W.: Semantic super-resolution for extremely low-resolution vehicle license plate. In: in Proc. IEEE Int. Conf. Acoust., Speech Signal Process. (ICASSP). pp. 3772–3776 (2019)